Power Distribution and Q-factor Analysis of Diffuse Cellular Indoor Visible Light Communication Systems

D. Wu*, Z. Ghassemlooy*, H. LeMinh*, S. Rajbhandari* and Y.S. Kavian**
*Optical Communication Research Group, School of CEIS, Northumbria University, Newcastle Upon Tyne, UK
**Faculty of Engineering, Shahid Chamran University, Ahvaz, Iran
E-mail: dehao.wu@northumbria.ac.uk

***Abstract*- Comparing with the existing incandescent, light-emitting diodes (LEDs) offer higher power efficiency, higher brightness, longer lifetime, and have a fast dynamic response in the order of a few megahertz. LEDs are recently expected to be utilised for the next generation indoor optical wireless communication (OWC) system. In this paper, we present a mathematical design model as well as a practical measurement for an indoor diffuse cellular visible light communication (VLC) system. It operates at a date rate of 5 Mb/s using the on-off keying non-return-to-zero (OOK-NRZ) modulation format. Using commercially available luminit holographic light shaping diffusers (LSD), we show that the achieved distributions of received power and the Q-factor are more uniform. The range and coverage area of the cellular link are therefore significantly extended.**

***Keywords*- Visible light communication, LED, power distribution, BER**

I. INTRODUCTION

Compared with the traditional incandescent and fluorescent lamps, LEDs have a number of advantages such as a longer life expectancy, a higher tolerance to humidity, a smaller size and lower power consumption. As the cost of manufacturing decreases, LEDs become affordable and popular for colour displays, traffic signals, and for illumination applications. In recent years, LEDs have been used to transmit data at higher rates over a short-range OWC link [1-3].

For dual purpose of illumination and data communications, white LEDs are ideal sources for future applications. With availability of highly efficient white LEDs (created by combining the prime colours: red, green, and blue) or by using a blue emitter in combination with a phosphor, we are witnessing a surge in research and development in indoor VLC systems [4, 5]. In this paper, we use the commercially popular (Luxeon Star/O) royal blue LED type as the transmitter.

The most common link configurations for indoor OWC systems are the line-of-sight (LOS) and the diffuse or a hybrid LOS-diffuse. Normally, the diffuse system provides a lager coverage area and an excellent mobility [6], but at the cost of lower data rates, higher path losses and multipath induced intersymbol interference (ISI) caused by the signal reflections from walls and other objects within the room. On the other hand, LOS links, where the beam is confined within a narrow field of view (FOV), offer a much higher channel capacity and a longer range [6]. However, LOS links offer a limited coverage area as well as requiring alignment and/or tracking to maintain link availability. To achieve higher data rates as well as a wider coverage area, a cellular system would be the preferred option.In this paper, a practical cellular indoor VLC link employing a blue LED as a transmitter is reported. In order to increase the cell coverage area with a uniform power distribution, holographic LSDs of different angles are employed.

The rest of the paper is organized as follow. In section II, characteristics of the transmitter, diffuser, channel and receiver are described. In section III, the experiment work is outlined followed by results and discussion. Finally, the conclusion is given in the last section IV.

II. SYSTEM DESCRIPTION

A. System Overview

The proposed indoor cellular VLC system is shown in Fig.1. LEDs are used both for lighting as well as communications. LED access points are connected to the backbone wired network via the ceiling. Communications for the entire room in the proposed system is covered by four optical cells, each of which has a wide divergence angle LED source. At the receiving end, the optical receivers, mounted on a mobile terminal, has a dedicated FOV of 30^0 to ensure seamless connectivity as well as alleviating the need for using pointing and tracking schemes. In addition the suitable modulation scheme can also be adopted to improve the overall system capacity.

Fig. 2 shows the proposed practical cellular indoor VLC link. The metallic frame has a dimension of $1.8\times1.5\times1$ m^3, which is divided into four compartments (or cells). Each cell consists of an LED transmitter, a diffuser and an optical receiver.

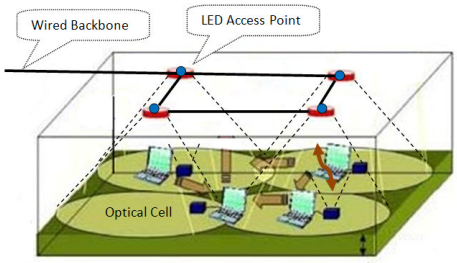

Fig. 1. Proposed indoor cellular VLC system

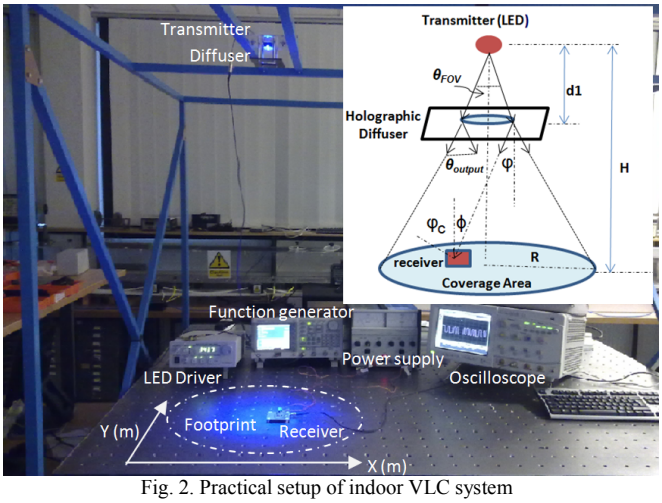

Fig. 2. Practical setup of indoor VLC system

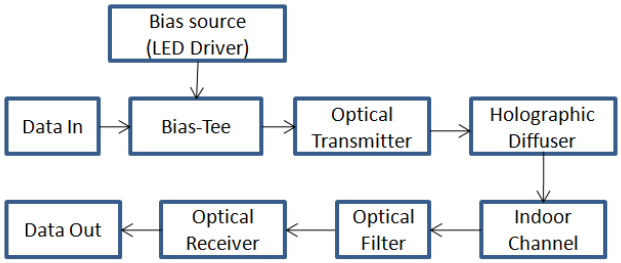

Fig. 3. A single cell VLC system diagram

The separation between the source and receiver is 1 m. In this paper, we only show the practical results for one cell at a data rate of 5 Mb/s using the OOK-NRZ modulation scheme.

B. *Transmitter*

LEDs, with no shaping lenses, can be essentially considered as the Lambertian source [3]. In many applications, however, there are requirements for specific radiation distributions to ensure a full coverage and an optimum link performance. In such cases shaping lenses are used at the transmitter. Here the light source position at the centre of a cell is composed of an LED and an optical lens. With the transmitter's full width at the half maximum angle (FWHM) of 7^{o} [7], the cell radius is 12.2 cm. This is equivalent to a coverage area of 474 cm^2. To achieve a wider coverage area with a uniform radiation distribution pattern, a luminit holographic LSD (10^0, 20^0, and 30^0) is employed. Fig. 3 depicts the system block diagram of a signal cell VLC system which includes a transmitter, a diffuser and a receiver.

C. *Model of Holographic LSD*

Using holographic LSD, the effective divergence angle of the transmitter can be extended, which can be calculated as [6]:

$$\theta_{output} \approx \sqrt{(\theta_{FOV})^2 + (\theta_{LSD})^2} \qquad (1)$$

where θ_{output} is the effective output angle of the light, θ_{FOV} is the light source FOV, and θ_{LSD} is the angle of LSD [7].

The hologram is a two level surface relief diffractive element that affects only the phase of light passing through it [8]. The far-field radiation pattern passing through the hologram is approximately the Fourier transform of the surface relief structure [9]. In order to simplify calculation of the beam intensity through the holographic LSD, as Fig. 4 shows, we have divided LSD into an array of 'pixels', and have used Matlab to simulate the beam profile for every 'pixel'. For a very tiny beam profile, the intensity of light can be considered as uniform after passing through the single 'pixel'. Finally, the overall coverage area is could be the sum of individual foot prints per pixel.

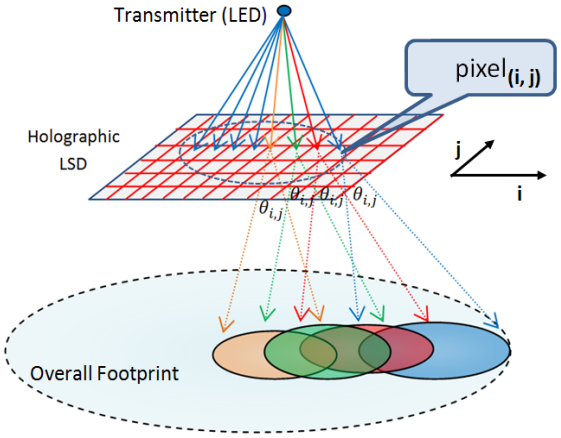

Fig. 4. Multiple beam profiles after holographic LSD

D. *Optical Wireless Channel*

Following the LOS link configuration adopted in [10], and assuming no optical filter and optical concentrator are used, the LOS channel DC gain is given by:

$$H(0) = \begin{cases} \frac{(m+1)A}{2\pi d^2}\cos^m(\phi)\cos(\varphi), & 0 \le \varphi \le \varphi_c \\ 0, & 0 \ge \varphi_c \end{cases} \qquad (2)$$

where A is the photodetector surface area, ϕ is the incidence angle, φ is irradiance angle, φ_c is the FOV (semiangle) at the receiver and H is the distance between transmitter and receiver. $= -\frac{\ln 2}{\ln(\cos\varphi_{1/2})}$ is the order of Lambertian radiant which is related to the transmitter semiangle $\varphi_{1/2}$, (at half power). The order m of the LED which we used is 110. The received power is given by:

$$P_{Rx} = P_{Tx}\, H(0) \qquad (3)$$

where P_{Tx} is the transmitted optical power of LED, P_{Rx} is the received optical power at the receiving plane.

E. Receiver

This receiver front-end consists of a commercial PIN junction photodetector and a trans-impedance amplifier. The specifications for the receiver are given in Table I.

TABLE I
SPECIFICATION FOR INDOOR VLC SYSTEM

LED product number	LXHL-NRR8
LED bandwidth	3.8 MHz
LED working wavelength	455 nm
LED output power	40 mW
LED field of view (FWHM)	14°
Diffuser	Luminit LSD 10°, 20° and 30°
Channel distance	1 m
Photodectector product number	OSD-15T
Photodectector detection area	15 mm^2
Photodectector responsivity	0.21 A/W at (λ=436 nm)
Photodectector rise time	12 ns
Preamplifier product number	AD8015
Preamplifier 3-dB bandwidth	240 MHz

III. RESULTS

The system specifications and parameters are given in Table I.

A. Simulated Results

We have used Matlab to simulate the optical power distribution of the indoor cellular OWC system. Using Eqs. (2) and (3), the normalized power distribution for a 4-cell structure (see Fig. 1) is illustrated in Fig. 5. Fig. 5 (b) is the contour of the power density at the receiving plane. It is can be seen that most of the power is concentrated near the centre of each cell decreasing sharply towards the cell edges. In a 4-cell configuration with a circular foot print, the area within dotted line circle, see Fig. 5(b), is defined as the 3-dB power attenuation area from the centre of a cell. The rest of the area is defined as the no coverage area or the 'dead zones' with no optical illumination. The over 3-dB coverage area A_{Cov}, where power attenuation is less than 3-dB for four cells is around 1800 cm^2, is given by:

$$A_{Cov} = \sum_{i=1}^{N} A_{cov_i} \tag{4}$$

where, N is the number of cells
The complete area of receiving plane is given by:

$$A_{Total} = A_{Cov} + A_{Dz} + A_{Ol} \tag{5}$$

where A_{Dz} and A_{Ol} shown in Fig. 5(b) are the 'dead zones' and the overlapping areas, respectively.

To achieve a uniform distribution within each cell, we have used a 30° LSD. Figs. 6 (a) and (b) display predicted power distributions and power density contours for a 4-cell configuration. The over 3-dB coverage area is marked in Fig. 6(b). Using Eq. (5), the total coverage area is around 8000 cm^2. Note the increase in the power distribution at the boundary regions because of cell overlapping.

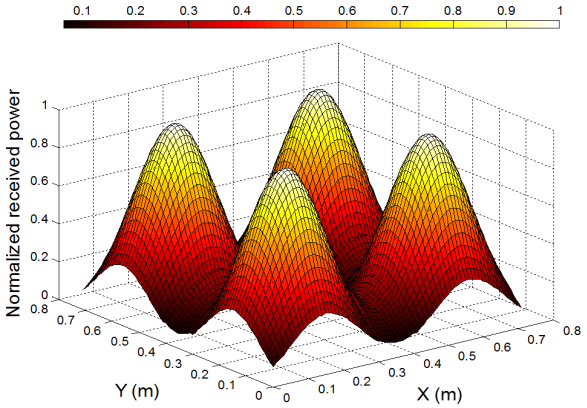

Fig. 5 (a). Predicted normalized power distribution at the receiving plane without LSD

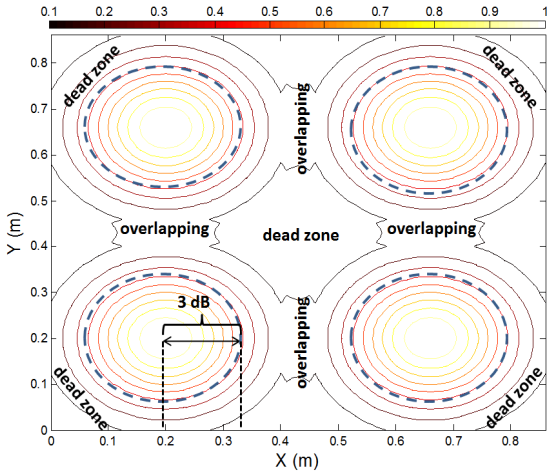

Fig. 5 (b). Predicted power contour plot at the receiving plane without LSD

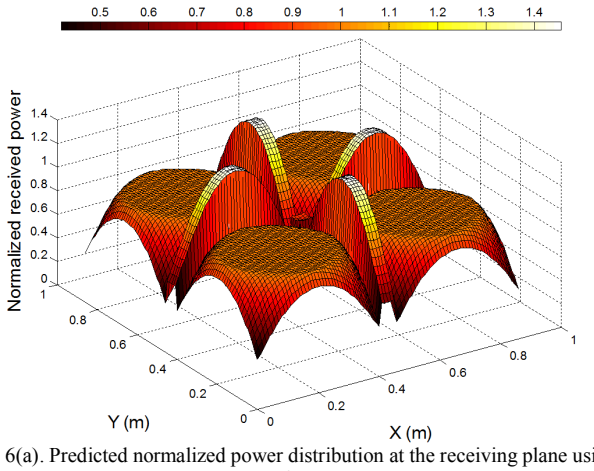

Fig. 6(a). Predicted normalized power distribution at the receiving plane using a 30° LSD

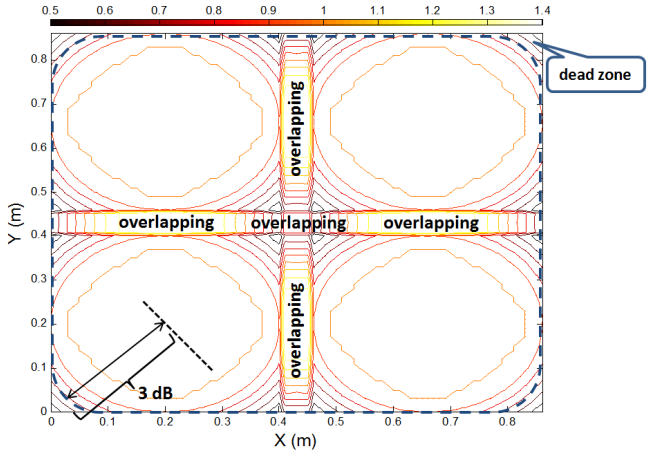

Fig. 6 (b). Predicted power contour plot at the receiving plane using a 30° LSD

B. *Practical Measurements*

Fig. 7 outlines the measured optical power distributions with and without holographic LSDs for a single cell configuration. The power density is more uniform when larger angle LSDs are used. Comparing the power density profiles of a link without a holographic LSD with a 30° holographic LSD (Figs. 7(a) and (d), it can be seen that a 3-dB transmission boundary has increased from 8 cm to 20 cm (i.e. 625% increasing in the coverage area).

Next we measured the eye diagrams for links with and without the holographic LSD in order to determine the Q-factor performance. Fig. 8 shows the 3D spatial distribution of the Q-factor. For the case with no LSD, Fig. 8(a), for a Q-factor > 5 corresponding to a BER < 10^{-6} (using OOK-NRZ modulation format), the effective coverage area is ~625 cm^2. The coverage area increases to ~ 1600 cm^2 using 30° LSDs.

As shown in Fig. 8 using wider angle LSDs, the Q-factor distribution is more uniform within a cell compared to the case with no LSD where the Q-factor is the highest at the cell centre.

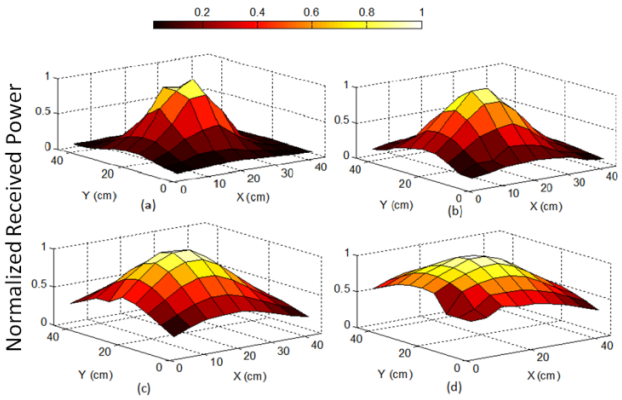

Fig. 7. Spatial distribution of received power: (a) without LSD, (b) with 10° LSD, (c) with 20° LSD, and (d) with 30° LSD

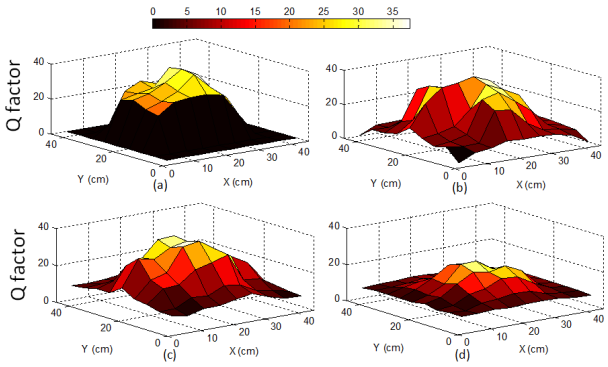

Fig. 8. Spatial distribution of Q factor: (a) without using LSD, (b) with 10° LSD, (c) with 20° LSD, and (d) with 30° LSD

IV. CONCLUSION

In this paper, we have modeled, simulated and measured the received power distributions for a practical indoor VLC link employing a holographic diffuser. The investigation showed that, using holographic LSDs with suitable angles, a uniform power distribution can be obtained thus increasing the coverage area in indoor VLC environment. This is a step forward to design a VLC cellular system.

ACKNOWLEDGMENT

I would like to acknowledge Dr David Johnston and Mr Andrew Burton for their help.

REFERENCES

[1] J.K, Kim and E.F. Schubert, "Transcending the replacement paradigm of solid-state lighting," *Optics Express,* vol. 16, no. 26, pp. 21835-21842, December 2008.

[2] Y. Tanaka, S. Haruyama, and M. Nakagawa, "Wireless optical transmissions with white colored LED for wireless home links," *Proc. IEEE International Symposium on Personal, Indoor and Mobile Radio Communications,* vol. 2, pp. 1325-1329, 2000.

[3] T. Komine and M. Nakagawa, "Fundamental analysis for visible light communication system using LED lights," *IEEE Trans. on consumer Electronics,* vol. 50, pp. 100-107, 2004.

[4] T. Komine, J.H. Lee, S. Haruyama and M. Nakagawa, "Adaptive equalization system for visible light wireless communication utilizing multiple white LED lighting equipment," *IEEE Trans. on wireless communications,* vol. 8, no. 6, pp. 1536-1276, 2009.

[5] H.L. Minh, *et al*, "100-Mb/s NRZ visible light communication using a post-equalized white LED," *IEEE Photonics Technology Letters,* vol. 21, no. 15, August 1, 2009.

[6] D.R. Wisely, "A 1 Gbit/s Optical Wireless Tracked Architecture for ATM Delivery," *IEE Colloquium on Optical Free Space Communication Links*, London, UK, 1996.

[7] Luminit, "Light Shaping Diffusers," Available at: http://www.luminitco.com/files/u1/Technical_Data_Sheet_rev_9-28-10.pdf (Accessed: 15 Jan 2011).

[8] P.L. Eardley, D.R. Wisely, D. Wood and P. McKee, "Holograms for Optical Wireless LANs," *IEE Proc. Optoelectron., Vol. 143, No. 6, December 1996.*

[9] M.Born and E. Wolf, "Principles of optics," *Pergamon Press*, 1986.

[10] J.M. Kahn and J.R. Barry, "Wireless infrared communication," *Proc. IEEE,* vol. 85, no. 2 pp. 265-298, 1997.